Stable sandwich structures of two-dimensional iron borides FeB$_x$ alloy: A first-principles calculation

Supplementary Material

Shao-Gang Xu[ab], Yu-Jun Zhao[a], Xiao-Bao Yang*[a], and Hu Xu*[b]

[a] Department of Physics, South China University of Technology, Guangzhou 510640, P. R. China

[b] Department of Physics, South University of Science and Technology of China, Shenzhen 518055, P. R. China
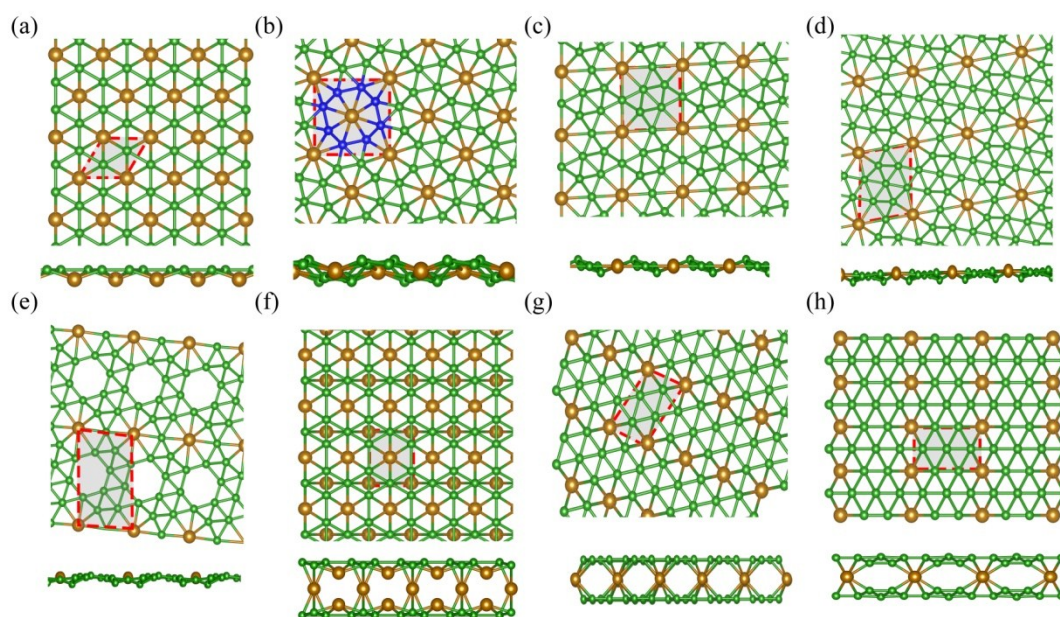
Fig.S1.The structure of the iron borides FeB$_x$ alloy(Top view and Side view). (a-e) The monolayer FeB$_x$($x=2^1$,4,6^2,8,10). (f-h) The sandwich structure FeB$_2$ and (Borophene FeB$_8$, FeB$_{10}$).

In order to measure the relative structural stability of all the structure with various coverage, we have calculated the formation enthalpy $\triangle H(x)$ as

$$\triangle H(x) = (E_{tot} - y \times \mu_{Fe} - x \times \mu_B)/(y + x)$$

The formation enthalpy phase diagram shown in the below.

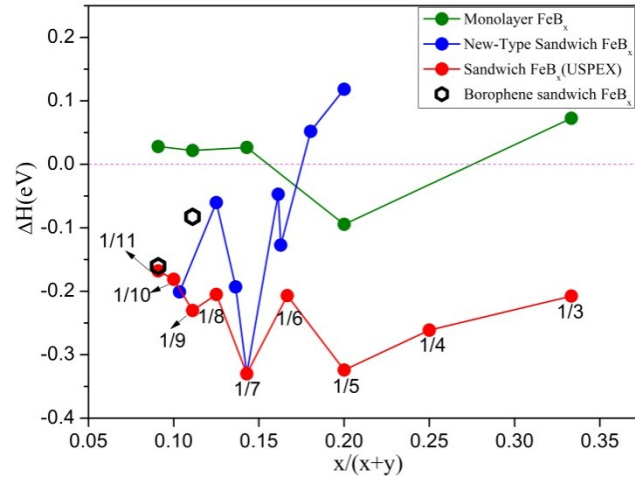*E-mail address: scxbyang@scut.edu.cn
*E-mail address: xu.h@sustc.edu.cn

Fig.S2. The formation enthalpy phase diagram with various coverage of iron borides FeB_x. The green dots represent the stable planar structure $FeB_x(x=2\text{-}10)$ search by USPEX. The red dots represent the stable sandwich FeB_x searched by USPEX. The blue dots represent the stable sandwich structures based on triangular lattice supercells. The two hollow hexagons represent the sandwich structure based on the borophene.
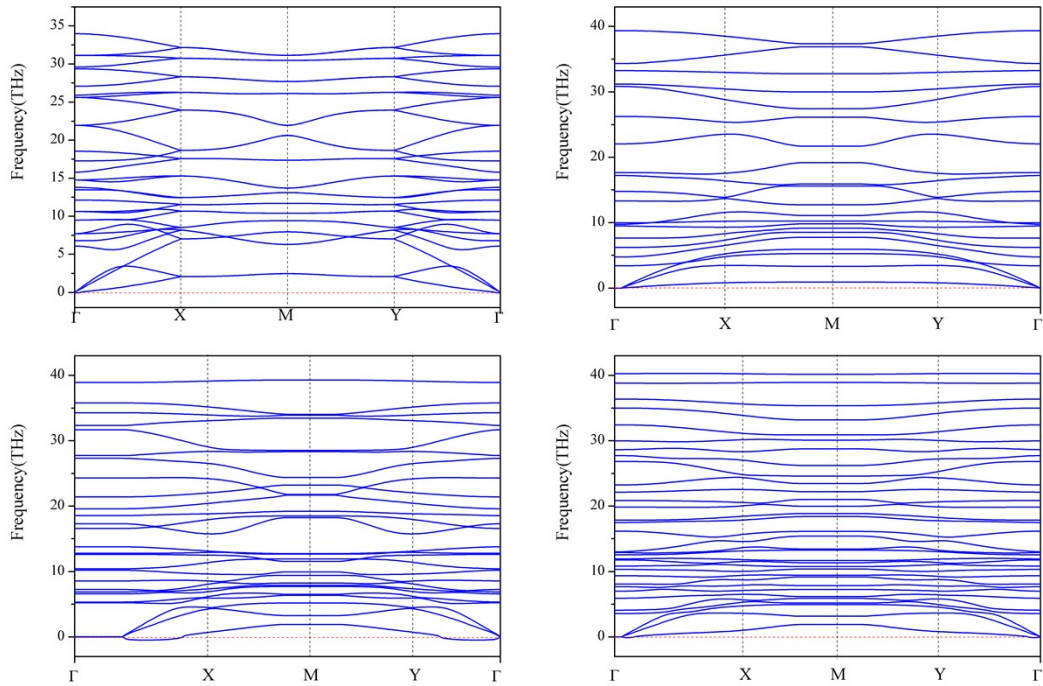

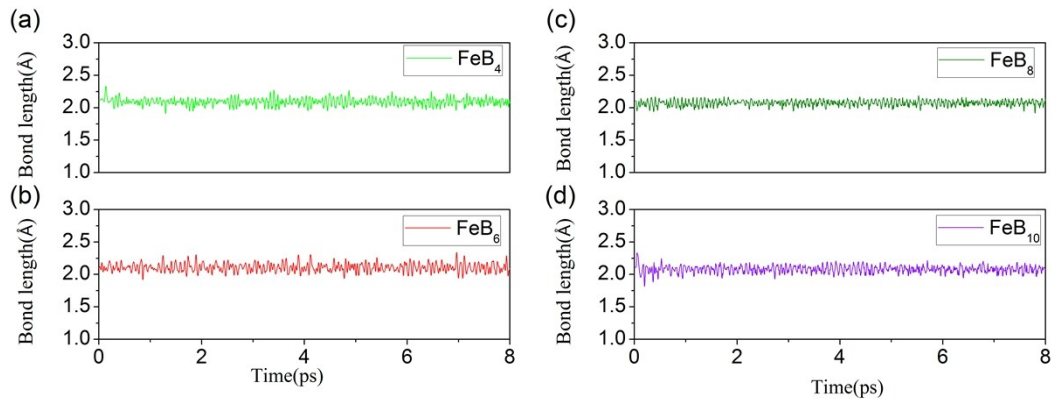Fig.S3. Phonon band dispersions of FeB_4, FeB_6, FeB_8 and FeB_{10} monolayer

Fig.S4. The Fe-B bond length fluctuation during AIMD simulations at 370K for the iron borides FeB_x(x=4,6,8,10) sandwiches(GGA-PBE).

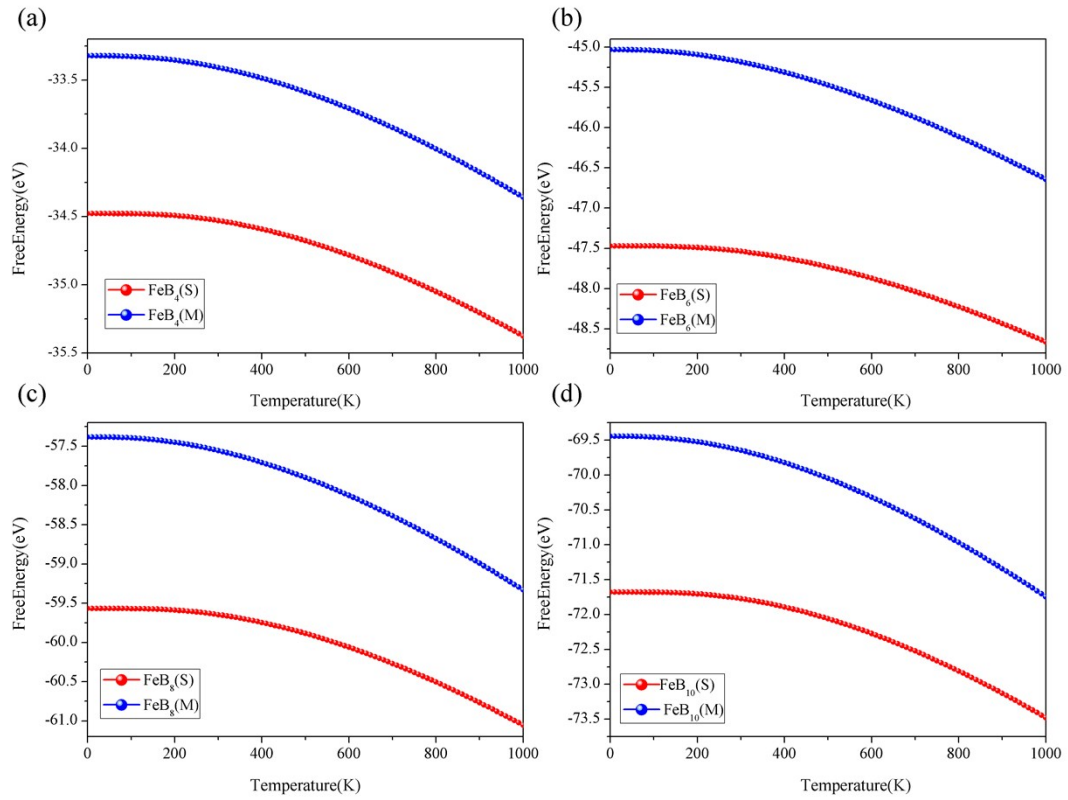Fig.S5. The free energies as a function of temperature for the corresponding iron borides FeB_x(x=4,6,8,10) alloies. The red dots represent the sandwich(S) structures, the blue dots represent the monolayer(M) structures, (a-d) shown the results of FeB_4, FeB_6, FeB_8 and FeB_{10}, respectively.
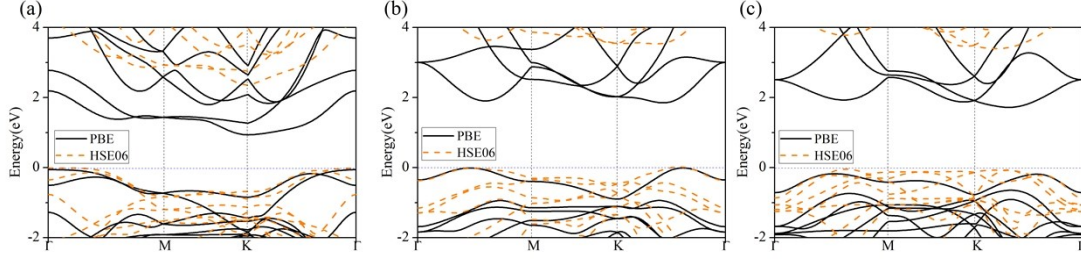
Fig.S6. (a,b,c) PBE and HSE06 band structures for FeB$_4$,FeB$_8$ and FeB$_{10}$ sandwichs.
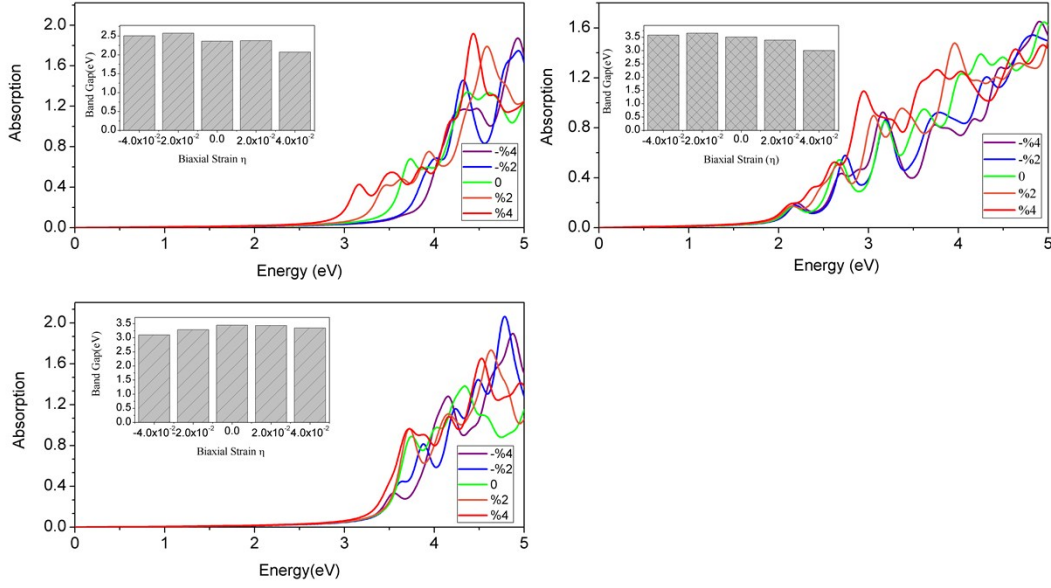

Fig.S7. The relation of optical properties and change of biaxial strain. (a-c) represent the results of FeB$_4$, FeB$_8$ and FeB$_{10}$ sandwichs based on the HSE06 functional.

The Raman active modes of the FeB$_6$ can be represneted by the Raman tensors in the group theory analysis, for point group symmetry D$_{6h}$, the Raman active modes are characterized by the following tensors (R):

$$A_{1g}:\begin{pmatrix} a & 0 & 0 \\ 0 & a & 0 \\ 0 & 0 & b \end{pmatrix} \qquad E_{1g}:\begin{pmatrix} 0 & 0 & 0 \\ 0 & 0 & c \\ 0 & c & 0 \end{pmatrix}\begin{pmatrix} 0 & 0 & c \\ 0 & 0 & 0 \\ c & 0 & 0 \end{pmatrix} \qquad E_{2g}:\begin{pmatrix} d & 0 & 0 \\ 0 & d & 0 \\ 0 & 0 & 0 \end{pmatrix}\begin{pmatrix} 0 & d & 0 \\ d & 0 & 0 \\ 0 & 0 & 0 \end{pmatrix}$$

The Raman scattering intensity is proportional to $|e_i \cdot R \cdot e_j|^2$, where e_i and e_s are the polarization vector of the incident light and scattering light, respectively, and R is the Raman tensor. If the materials are oriented in the xy plane, the incoming and scattered lights are oriented along the z axis. Here the vector e_i and e_s can be written as $(\cos\theta,\sin\theta,0)$ and $(\cos\alpha,\sin\alpha,0)$ respectively. While, in the backscattering configuration the modes A$_{1g}$ and E$_{1g}$ do not contribute to the Raman spectra.

Here, the intensity of mode E$_{2g}$(a) is calculated as $I_{E_{2g}}(a) \approx d^2|cos(\theta - \alpha)|^2$, and mode E$_{2g}$(b) is calculated as $I_{E_{2g}}(b) \approx d^2|sin(\theta + \alpha)|^2$. As the in-plane rotation of the crystal by φ is equivalent to the rotation of both

4

incoming and scattered light by -φ with sample fixed. We applied the simplified situation with the parallel

polarization (θ=α), and then rotate the sample by φ, then $I_{E_{2g}}(a) \approx d^2$, $I_{E_{2g}}(b) \approx d^2 sin^2(2\varphi)$.

For $E_{2g}(a)$ mode, the material would be isotropic, with a constant radial dependence. The $E_{2g}(b)$ with angular dependence for the intensity, which reaches a minimum when φ =0°,90°,180°, and 270°, otherwise, φ =45°,135°,225° and 315° meet the maximum, which is shown in Fig.S8.
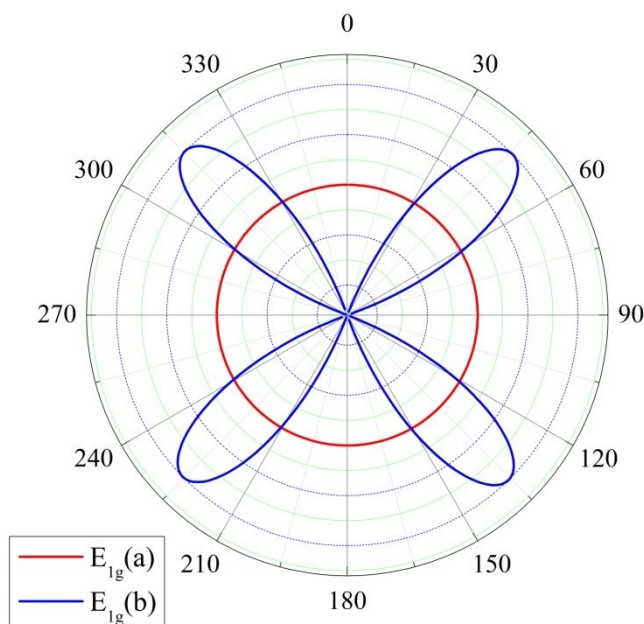
Fig.S8. Angular dependence of Raman intensity for FeB_6 with D_{6h} symmetry. The polarization dependence for $E_{1g}(a),(b)$.

Direct coordinates for the stable iron borides $FeB_x(x=4,6,8,10)$ sandwiches. (POSCAR)

\#

FeB₄

B Fe

  1.00000000000000

    1.7773000000000001   -3.0783000000000000   0.0000000000000000

    1.7773000000000001   3.0783000000000000   0.0000000000000000

    0.0000000000000000   0.0000000000000000   18.0281610000073513

   B   Fe

    8   2

Direct

  0.6524543516174219 0.9796620202595889 0.5000019245420333

  0.1524544523619511 0.4796619195150598 0.5000020754579708

```
0.1524309043532739    0.4796776747562532    0.3843698326241096
0.6524313479881911    0.9796791344540310    0.6156267908845621
0.6524447219481218    0.4796671660658305    0.6161818717156038
0.1524444478427540    0.9796658919604582    0.3838171282843987
0.6524442793638627    0.9796866057100573    0.3843721037653722
0.1524437390616455    0.4796870493449674    0.6156292727259611
0.6524027996541406    0.4796996908896247    0.4479376594237223
0.1524029558086397    0.9796998470441238    0.5520623405762777
```

###

FeB$_6$

B Fe
```
   1.00000000000000
     3.4748999999999999      0.0000000000000000      0.0000000000000000
    -1.7374499999999999      3.0093519999999998      0.0000000000000000
     0.0000000000000000      0.0000000000000000     15.1183004379000003
   B     Fe
   6      1
Direct
  0.0000000000000000    0.5000000000000000    0.4221512269607146
  0.0000000000000000    0.5000000000000000    0.5778488030392879
  0.5000000000000000    0.5000000000000000    0.4221512269607146
  0.5000000000000000    0.5000000000000000    0.5778488030392879
  0.5000000000000000    0.0000000000000000    0.4221512269607146
  0.5000000000000000    0.0000000000000000    0.5778488030392879
  0.0000000000000000    0.0000000000000000    0.5000000000000000
```

###

FeB$_8$

POSCAR B   Fe
```
   1.00000200000000
     1.7295339605100899     -2.9955528196034802      0.0000000000000000
     1.7295339605100899      2.9955528196034802      0.0000000000000000
     0.0000000000000000      0.0000000000000000     17.9915770006009694
   B     Fe
   8      1
Direct
  0.5303370235417333    0.0109324390426195    0.5328991254036808
  0.0303412995273078    0.5109335605626129    0.5328995111860095
  0.5303455775325858    0.5109360137850771    0.5329009851771715
  0.6969572911344315    0.3442318601859995    0.6180212733945254
  0.0303249205141753    0.5110188954788271    0.3997071340647054
  0.5303291456159087    0.5110228895649769    0.3997068427882127
  0.5303265566221995    0.0110285005609114    0.3997086747461154
```

0.3636379204224767   0.6775902258135176   0.6180220819886770

0.0303442650891981   0.0109996150054457   0.4661373712508876

##

FeB$_{10}$

```
POSCAR   B   Fe
   1.00000200000000
     1.7295339605100899    -2.9955528196034802     0.0000000000000000
     1.7295339605100899     2.9955528196034802     0.0000000000000000
     0.0000000000000000     0.0000000000000000    17.9915770006009694
    B      Fe
    10      1
Direct
  0.5303845845688997   0.0110683574548389   0.5333523099667090
  0.0303827297054085   0.5110642025026806   0.5333500018896160
  0.5303815820558881   0.5110650643083261   0.5333518147173706
  0.6970479116897721   0.3443479512786354   0.6184741507909308
  0.0302674947380481   0.5108835762893449   0.3992222733144430
  0.5302747412859503   0.5108850457444447   0.3992207599283617
  0.5302671331367321   0.0108753088481777   0.3992344400428181
  0.3636920425430503   0.6776674579012862   0.6184787854246068
  0.6968698656190568   0.3440659418876209   0.3141026518478327
  0.3636235818599047   0.6775919975243809   0.3140941611744594
  0.0303475443542141   0.0110011822597613   0.4662898509028395
```

##

Reference

1.   H. Zhang, Y. Li, J. Hou, A. Du and Z. Chen, *Nano Lett.*, 2016, 16, 6124-6129.

2.   H. J. Zhang, Y. F. Li, J. H. Hou, K. X. Tu and Z. F. Chen, *J. Am. Chem. Soc.*, 2016, 138, 5644-5651.